HHS Public Access

Author manuscript

Methods Mol Biol. Author manuscript; available in PMC 2024 June 14.

Published in final edited form as:

Methods Mol Biol. 2024 ; 2800: 189–202. doi:10.1007/978-1-0716-3834-7_13.

Reconstructing signaling networks using biosensor barcoding

Suyang Wang[1,5], **Wei-Yu Chi**[1,5,*], **Gabriel Au**[2], **Cheng-Chieh Huang**[1], **Jr-Ming Yang**[1,†], **Chuan-Hsiang Huang**[1,3,4,†]

[1]Department of Pathology, Johns Hopkins Medical Institutions, Baltimore, MD 21205, USA

[2]Department of Biology, Krieger School of Arts and Sciences, Johns Hopkins University, Baltimore, MD 21218, USA

[3]Department of Cell Biology, School of Medicine, Johns Hopkins University, Baltimore, MD 21205, USA

[4]Center for Cell Dynamics, School of Medicine, Johns Hopkins University, Baltimore, MD, USA

[5]These authors contributed equally to this work.

Summary

ii.

Understanding how signaling networks are regulated offers valuable insights into how cells and organisms react to internal and external stimuli and is crucial for developing novel strategies to treat diseases. To achieve this, it is necessary to delineate the intricate interactions between the nodes in the network, which can be accomplished by measuring the activities of individual nodes under perturbation conditions. To facilitate this, we have recently developed a biosensor barcoding technique that enables massively multiplexed tracking of numerous signaling activities in live cells using genetically encoded fluorescent biosensors. In this chapter, we detail how we employed this method to reconstruct the EGFR signaling network by systematically monitoring the activities of individual nodes under perturbations.

Keywords

Genetically encoded fluorescent biosensors; live cell imaging; signaling network; deep learning; receptor tyrosine kinases (RTKs); epidermal growth factor receptor (EGFR); multiplexing; small molecule inhibitors

1. Introduction

Numerous biochemical activities are responsible for coordinating cellular functions in both space and time. To track these activities in live cells, many genetically encoded fluorescent biosensors have been developed utilizing fluorescent proteins (FPs). These biosensors allow for the monitoring of various cellular activities, such as signaling and metabolic processes [1]. However, the limited spectral space and broad emission spectra of FPs have prevented

†Correspondence: chuang29@jhmi.edu (C.-H.H.), jyang38@jhmi.edu (J.-M.Y.).
*Present address: Weill Cornell Medicine, New York, NY 10065, USA

the imaging of more than a few biosensors in a single experiment, despite attempts to increase multiplexity. One such attempt includes expanding the color spectrum of biosensors or targeting them to different intracellular sites [2]. However, these strategies have limited success in expanding the number of activities to be monitored, as no more than 5–6 different biosensors can be imaged at the same time. To overcome the limitation of imaging only a few biosensors in a single experiment, we recently introduced a method for massively multiplexed biosensor imaging [3,4]. Our approach, known as "biosensor barcoding," involves labeling cells expressing different biosensors with barcodes consisting of a pair of barcoding proteins - blue or red fluorescent proteins that are targeted to distinct subcellular locations (Fig. 1A, B). Unlike the commonly used cyan, green, or yellow FPs in biosensors, the emission spectra of the barcoding proteins are easily separable. Following cell mixing, spectral images of the barcodes are obtained at the beginning of the experiment, followed by time-lapse imaging of biosensors (Fig. 1C) using a fluorescent microscope equipped with a spectral detector. The barcode present in each cell allows for the identification of the biosensor expressed, which can be achieved using machine learning models. Subsequently, the signals of cells expressing the same biosensor can be combined for further analysis (Fig. 1D). Information from the responses to perturbations can reveal the regulatory structure of signaling networks (Fig. 1E).

Besides improving the efficiency of data acquisition, the biosensor barcoding method has other benefits. Firstly, cells expressing various biosensors exhibit synchronized activities, which simplifies the comparison of different biosensors. Secondly, the capability to label distinct cell populations in the same mixture enables differentiation between cell-autonomous and non-autonomous effects [3].

By enabling massively parallel imaging of biosensors, our method provides a powerful tool for reconstructing signaling networks. Specifically, we can use the method to track the activities of individual nodes in the signaling network and observe their responses when the nodes are individually blocked using small molecule inhibitors. In this chapter, we demonstrate this strategy using the EGFR signaling network as an example (Fig. 2), but the strategy can be easily applied to the study of other signaling networks.

2. Materials

2.1 Cell culture and transfection

1. HeLa cells are purchased from ATCC (CCL2).
2. Accutase cell detachment solution (Sigma)
3. DPBS (Dulbecco's phosphate-buffered saline)
4. Culture Medium: DMEM, with L-glutamine and high glucose, supplemented with 10% FBS, 1 mM sodium pyruvate and 1X MEM non-essential amino acids.
5. Imaging Medium: DMEM, with L-glutamine and high glucose, HEPES, no phenol red, supplemented with 10% FBS, 1 mM sodium pyruvate and 1X MEM non-essential amino acids.

6. GenJet™ In Vitro DNA Transfection Reagent (Ver. II)

2.2 Plasmids

Barcoding proteins used in this chapter include the following (see Table 1 for an explanation of the barcoding protein nomenclature):

1. D1: BFP-NLS, Addgene #184458
2. D2: BFP-CAAX, Addgene #184459
3. B1: mCardinal-NLS, Addgene #184450
4. B3: mCardinal-LaminB1, Addgene #184452
5. B4: mCardinal-NES, Addgene #184453
6. C1: iRFP702-NLS,: Addgene #184454
7. C2: iRFP702-CAAX, Addgene #184455
8. C4: iRFP702-NES, Addgene #184457
9. E2: mCherry-CAAX, Addgene #186347
10. E3: mCherry-LaminB1, Addgene #186348
11. E4: mCherry-NES, Addgene #186349

Biosensors:

1. PicchuEV [5]
2. RhoA2G, Addgene #40176 [6]
3. Lyn-FAK biosensor, Addgene #78299 [7]
4. Cytosolic Syk Biosensor, Addgene #125729 [8]
5. PH-AKT-GFP, Addgene #51465 [9]
6. Cytoplasmic EKAR (Cerulean-Venus), Addgene #18679 [10]
7. GCaMP6s, Addgene #40753 [11]
8. EV-ROCK [12]
9. Src biosensor, Addgene #78302 [13]
10. EV-S6K [5]

2.3 Chemicals

1. DMSO: vehicle control
2. Gefitinib: EGFR inhibitor
3. PF562271: FAK inhibitor
4. ZSTK474: PI3K inhibitor
5. GDC-0994: ERK inhibitor

6. BAPTA: Calcium chelator
7. Y27632: ROCK inhibitor
8. Dasatinib: Src inhibitor
9. LY2584702: S6K inhibitor

See also Table 2.

2.4 Imaging equipment

1. Zeiss AxioObserver with 780-Quasar confocal module, which is equipped with a 34-channel high-sensitivity gallium-arsenide phosphide (GaAsP) spectral detector controlled by the Zen software.
2. Three laser excitation wavelengths are used: 405 nm for BFP, 458 nm for CFP/GFP/YFP, and 633 nm for the red FPs. The emission signals of BFP, CFP, YFP/GFP and red FPs are collected in the ranges of 371–430 nm, 458–499 nm, 508–543 nm, and 561–695 nm, respectively. (Note 1)
3. An environmental control chamber maintains the cells at 37°C during time-lapse imaging. The microscope is also equipped with a motorized stage for multi-position image acquisition, and a Definite Focus module for auto-focusing.

2.5 Image analysis software

1. ImageJ/Fiji (https://imagej.net/software/fiji/) [14,15]
2. Python 3 https://www.python.org
3. Keras https://keras.io/ [16]
4. TensorFlow https://www.tensorflow.org/ [17]
5. Scripts and deep learning models for analysis can be downloaded from: https://github.com/BearHuangLab/Biosensor-barcoding

3. Methods

3.1 Transfection of HeLa cells with biosensors and barcodes

1. Day 1, seed 2×10^5 HeLa cells to 10 wells in a 12-well tissue culture plate along with 2 mL of DMEM complete medium. Incubate the cells overnight at 37°C, 5% CO_2. (see Note 2)
2. Day 2, replace the medium in each well with 0.75 mL of fresh DMEM complete medium 30 minutes prior to transfection.
3. For each well, prepare one tube of diluted DNA solution and one with the GenJet™ transfection reagent. First, dilute 0.75 μg of DNA in 38 μL of serum-free DMEM. In each transfection, the DNA mixture contains two barcoding proteins and one biosensor (Table 1). Start with a mass ratio of 1:1:1 and adjust the ratio if necessary to achieve optimal fluorescence signal (Note 3). Next for the transfection reagent, add 2.25 μL GenJet™ Transfection Reagent in 38 μL of

serum-free DMEM. Mix by vortexing and spin down briefly. Immediately add the diluted transfection reagent to the diluted DNA solution, and pipette up and down a few times to mix. Leave the mixture at room temperature for 15 min.

4. Add the DNA-GenJet™ complex dropwise to cells in the 12-well plate. Incubate cells at 37°C, 5% CO_2 overnight.

5. Day 3, collect the cells by removing the medium containing DNA-GenJet™ complex. Rinse each well with DPBS, apirate, and detach the cells with Accutase. Mix cells from all 10 wells together and resuspend with Imaging Medium. Seed 5×10^5 cells in 35 mm glass-bottom dishes, and incubate overnight at 37°C, 5% CO_2.

3.2 Live cell imaging

3.2.1 Imaging barcodes with Zeiss LSM780-FCS laser scanning confocal microscope

1. Before imaging, replace the medium with fresh Imaging Medium for each dish.

2. Turn on the microscope, halogen lamp, and argon laser. Switch the objective to the 40X oil lens and add a small drop of immersion oil. Place the glass-bottom dish on the stage. Remove the culture dish lid for accessible drug administration during time-lapse imaging experiments. Secure the dish with stage clips.

3. Open the Zen software on the computer and turn on the stage incubator to 37°C. Select the “Locate” setting on the software and switch on “Transmitted light”. Locate cells by adjusting microscope focus.

4. Switch to “Acquisition” and select the “Lambda Mode” tab under “Light Path”. For the far red barcodes select the 633 nm laser as the excitation source and set the pinhole size to 30.2. Set range to 561–695 nm with resolution of 8.9 nm (Note 4).

5. To capture images, choose 30 positions containing at least 6–10 cells with strong fluorescent signals in each view field. Save the barcode images as *[Experiment ID]*_633Ex.lsm. (see Note 5).

6. To differentiate the red barcodes, perform Linear Unmixing using the reference spectra to generate three separate images (mCherry, mCardinal and iRFP702) for each position (the reference spectra can be obtained using cells expressing individual FPs; see (Chi et al. 2022) for details). Save the file as *[Experiment ID]*_633Ex_Linear unmixing.lsm.

7. For the BFP barcode, acquire images through “Channel Mode”. Select the 405 nm laser as the excitation source and set range to 371–430 nm with pinhole size of 30.2. Save the file as *[Experiment ID]*_405Ex.lsm.

3.2.2 Imaging cells treated with inhibitors

1. After the barcode images are captured, start time-lapse imaging for biosensor responses. For drug inhibition studies, time-lapse images are taken for each position every 3 min for 10 frames in total.
2. On the Zen software, click the “Channel Mode” tab under “Light Path” selections. To capture FRET and KTR biosensors, select the spectrum range of 458–499 nm (for CFP) and 508–543 nm (for YFP and GFP). For the excitation source, use the 458 nm laser and set the pinhole size to 300.6.
3. Select “Time Series”. Set the frame rate at 3 min per frame for 10 frames, and choose “Definite Focus” as the focusing strategy.
4. Immediately after acquiring 3 images (frame 3) for all positions, add the inhibitor (see Table 2 for the list of inhibitors) by carefully lifting the incubator lid and gently add the reagents to the dish.
5. When imaging is done, save the file as *[Experiment ID]*_FRET.lsm.
6. Save the four files (see Table 3) generated from each imaging experiment to a separate folder without other files. This is needed for the macros to correctly identify the files.

3.3 Image analysis

3.3.1 Identifying barcodes using ImageJ

1. Download and install necessary programs and files: ImageJ Fiji from https://imagej.net/software/fiji/, Python 3 from https://www.python.org/, and necessary scripts and files developed by our lab from https://github.com/BearHuangLab/Biosensor-barcoding.
2. Open Fiji. Open the image file ending with “FRET.lsm” by dragging it onto the ImageJ toolbar.
3. Next, open the ImageJ macro titled “2. Barcode identification/Image Analysis.ijm” for barcode selection.
4. In the macro window, select “Run” and enter the number of positions in the images and time points per position. Click “OK” to continue.
5. After clicking “OK,” the “FRET.lsm” file will be split into two image windows: “combined-YFP” and “combined-CFP”, and a dialog box will prompt the user to select ROIs. DO NOT click OK until all ROIs are selected.
6. Use the selection tools to circle cells with visible fluorescence in the “combine-YFP” window. Adjust the contrast to see cells of low intensity. Individually outline each cell by using the oval select tool and pressing “T” to record the position of the cell into the ROI manager. Each circled area should include only one cell. Scroll across all time points to make sure that cells remain in the circled region (See Note 6). Click “OK” on the dialogue box when finished.

7. The macro will then prompt the user to enter the experiment name. Enter a name (e.g. “YYYYMMDD HeLa Cells”) and press enter. The macro will proceed to collect data for each cell and write it to files in the experiment folder.

8. Before analysis with the deep learning models, create a list of barcodes to classify by editing the barcode list file (*Barcode identification> Barcode reading GUI> Barcode list.txt*).

9. To automatically classify each fluorescent barcode, run the script “Barcode.py” to open the Barcode Prediction GUI. To run the script, open a command line, and type “python” followed by the path to your script, i.e., > python ./ path_to_your_script/preprocess barcode.py

10. In the GUI, select and load or confirm the prediction models, the barcode list, barcode image folder (“Barcodes” in experiment folder), and spectral data (***_spectrumdata.txt in experiment folder) (Note 7). Edit the output directory if desired. Click “Predict barcode” to generate a file called “modelpred.csv” containing the predicted barcode for each cell.

11. For best results, single-fluorophore biosensors GCaMP6S and PH-AKT should have their ROIs shrunk to include only the cell after classification. For PH-AKT, only the cytosol should be included. This can be done by opening combined-YFP.tif and ***_FRET_ROISet.zip from the experiment folder in ImageJ, shrinking the ROI of each cell with a single-fluorophore, and recording the intensity *More> Multi-Measure> Ok* in the ROI Manager. The resulting intensity data should be pasted to overwrite the YFP data in the *** _ROIData.csv file (also in experiment folder). This step can also be done using the macro *Barcode identification> “PH-AKT Reprocessing.ijm”*.

3.3.2 Analysis of biosensor response

1. Open the Excel template *Analysis> “10Mix_Template_STAR_Protocols.xlsx”*.

2. Switch to the sheet “Barcodes” and edit the barcode-biosensor combinations if needed.

3. Switch to the sheet “All_Cells” and copy over the biosensor classification and signal data. From the barcode prediction output (modelpred.csv), copy the columns [Index] and [Thresholded] to the template columns [Position] and [Barcode], respectively. From the file ***_ROIdata.csv in the experiment folder, copy the raw fluorophore data and transpose paste (in Excel *Right Click> Paste Options> Transpose (T)*) into the template columns [YFP1]...[CFP10]. Do not copy any row or column headers from data files. The activities will be calculated automatically.

4. The final result will be in the sheet “Analysis”. The activities are normalized to the average of those in the prestimulus levels, and biosensors with “inverted” design (i.e. less FRET or fluorescence when active) have the raw signal inverted so that the displayed signal directly corresponds to activity. In other words, the activities represent YFP/CFP for PicchuEV, RhoA-2G, EV-ROCK, EKAR,

and EV-S6K; CFP/YFP for Syk, Src, and Lyn-FAK; cytosolic fluorescence (GCaMP6S); and 1/cytosolic fluorescence (PH-AKT).

3.4 Generation of interaction map

By analyzing the biosensor responses to inhibitors, we can deduce how the nodes in the network interact with each other. For instance, when compared to the responses to the vehicle control (DMSO), the use of the FAK inhibitor led to a significant decrease in the activity of FAK, Src, and ERK, while increasing the activity of RhoA (Fig. 3A). This suggests that FAK has a positive interaction with Src and ERK, but a negative interaction with RhoA (Fig. 3B). To construct a comprehensive interaction map for the EGFR signaling network, we compare the biosensor responses to all inhibitors with those of the vehicle control (Fig. 4A). This analysis comprised the following steps:

1. Calculate the **Total Activity Score (TAS)** of each cell by summing up the activity (from section 3.3.2) across all time points.
2. For each inhibitor experiment, compare the TAS of cells expressing specific biosensor (inferred from the barcode) with the TAS of the same biosensor in the DMSO control experiment using Student's t test to get the significance (p values).
3. The effects of inhibitors on biosensors can be represented by the matrix of inhibition, in which the value of each element is calculated by: −log(p-value) × direction of change (i.e. +1 for positive effects; −1 for negative effects (Fig. 4B).
4. Generate the interaction diagram based on the matrix of inhibition. As explained above (Fig. 3), positive and negative interactions are assigned for inhibitory and activating effects, respectively (Fig. 4C).

Concluding remarks

The interaction map that has been created serves as a valuable tool for future investigations of the EGFR signaling network and for identifying novel interactions within signaling networks of specific cells. However, it is important to consider that certain interactions may be indirect or influenced by unintended effects of the inhibitors, and could vary depending on the cell type being studied. Nonetheless, these findings emphasize the intricate regulatory connections between nodes in the EGFR signaling network and demonstrate an effective approach to uncovering previously unknown interactions within signaling networks of specific cell types.

4. Notes

Note 1. GFP and YFP are both imaged under the excitation laser for CFP (458 nm). In some publications, the YFP channel is labeled as the FRET channel, and the YFP/CFP ratio as the FRET/CFP ratio.

Note 2. In order to optimize your transfection process, it is recommended to work with healthy cells that have undergone only a few passages. Regular maintenance of the cells is

also important to prevent overcrowding. When it comes to transfection, it is best to aim for a cell density of 70%–80%.

Note 3. If the barcode signal is too low, increase the DNA amount during transfection. Additionally, make sure to use high-quality plasmid DNA that is free from phenol, sodium chloride, and endotoxins.

Note 4. During focus adjustment or cell search, it is recommended to lower the laser power, minimize exposure time, and utilize RFP instead of BFP due to its susceptibility to quick bleaching.

Note 5. Depending on the velocity of the motorized stage and the time interval between consecutive image frames, the number of positions can be adjusted to optimize the number of cells captured and permit ample time for both image acquisition and EGF administration.

Note 6. If it proves challenging to encompass the entire cell within the chosen region, try incorporating a portion of the nucleus and plasma membrane. In addition, exclude apoptotic cells, debris, or impurities from the area of interest.

Note 7. The thresholds for models 2 and 3 are both set to 0.9 by default. While a greater threshold typically results in more precise outcomes, it also has the tendency to recognize fewer cells.

Acknowledgments

The plasmids of PicchuEV, EV-ROCK, and EV-S6K were provided by Michiyuki Matsuda, to whom the authors extend their gratitude. This work was supported by funding from R01GM136711 (to C.H.H.), Cervical Cancer SPORE P50CA098252 Career Development Award (to J.M.Y.) and Pilot Project Award (to C.H.H.), the W. W. Smith Charitable Trust (#C1901, to C.H.H.) and the Sol Goldman Pancreatic Cancer Research Center (to C.H.H.). Additionally, the purchase of the Zeiss LSM 780 confocal microscope was made possible by NIH grants S10OD016374.

5. References

1. Greenwald EC, Mehta S, Zhang J. Genetically Encoded Fluorescent Biosensors Illuminate the Spatiotemporal Regulation of Signaling Networks. Chem Rev. 2018;118: 11707–11794. doi:10.1021/acs.chemrev.8b00333 [PubMed: 30550275]
2. Terai T, Campbell RE. Barcodes, co-cultures, and deep learning take genetically encoded biosensor multiplexing to the nth degree. Mol Cell. 2022;82: 239–240. doi:10.1016/j.molcel.2021.12.017 [PubMed: 35063093]
3. Yang J-M, Chi W-Y, Liang J, Takayanagi S, Iglesias PA, Huang C-H. Deciphering cell signaling networks with massively multiplexed biosensor barcoding. Cell. 2021;184: 6193–6206.e14. doi:10.1016/j.cell.2021.11.005 [PubMed: 34838160]
4. Chi W-Y, Au G, Liang J, Chen C-C, Huang C-H, Yang J-M. Imaging and analysis for simultaneous tracking of fluorescent biosensors in barcoded cells. STAR Protoc. 2022;3: 101611. doi:10.1016/j.xpro.2022.101611 [PubMed: 36042884]
5. Komatsu N, Aoki K, Yamada M, Yukinaga H, Fujita Y, Kamioka Y, et al. Development of an optimized backbone of FRET biosensors for kinases and GTPases. Mol Biol Cell. 2011;22: 4647–4656. doi:10.1091/mbc.E11-01-0072 [PubMed: 21976697]
6. Fritz RD, Letzelter M, Reimann A, Martin K, Fusco L, Ritsma L, et al. A versatile toolkit to produce sensitive FRET biosensors to visualize signaling in time and space. Sci Signal. 2013;6: rsá12. doi:10.1126/scisignal.2004135

7. Seong J, Ouyang M, Kim T, Sun J, Wen P-C, Lu S, et al. Detection of focal adhesion kinase activation at membrane microdomains by fluorescence resonance energy transfer. Nat Commun. 2011;2: 406. doi:10.1038/ncomms1414 [PubMed: 21792185]

8. Xiang X, Sun J, Wu J, He H-T, Wang Y, Zhu C. A FRET-Based Biosensor for Imaging SYK Activities in Living Cells. Cell Mol Bioeng. 2011;4: 670–677. doi:10.1007/s12195-011-0211-x [PubMed: 25541586]

9. Várnai P, Balla T. Visualization of phosphoinositides that bind pleckstrin homology domains: calcium- and agonist-induced dynamic changes and relationship to myo-[3H]inositol-labeled phosphoinositide pools. J Cell Biol. 1998;143: 501–510. doi:10.1083/jcb.143.2.501 [PubMed: 9786958]

10. Harvey CD, Ehrhardt AG, Cellurale C, Zhong H, Yasuda R, Davis RJ, et al. A genetically encoded fluorescent sensor of ERK activity. Proc Natl Acad Sci U S A. 2008;105: 19264–19269. doi:10.1073/pnas.0804598105 [PubMed: 19033456]

11. Chen T-W, Wardill TJ, Sun Y, Pulver SR, Renninger SL, Baohan A, et al. Ultrasensitive fluorescent proteins for imaging neuronal activity. Nature. 2013;499: 295–300. doi:10.1038/nature12354 [PubMed: 23868258]

12. Li C, Imanishi A, Komatsu N, Terai K, Amano M, Kaibuchi K, et al. A FRET Biosensor for ROCK Based on a Consensus Substrate Sequence Identified by KISS Technology. Cell Struct Funct. 2017;42: 1–13. doi:10.1247/csf.16016 [PubMed: 27885213]

13. Ouyang M, Sun J, Chien S, Wang Y. Determination of hierarchical relationship of Src and Rac at subcellular locations with FRET biosensors. Proc Natl Acad Sci U S A. 2008;105: 14353–14358. doi:10.1073/pnas.0807537105 [PubMed: 18799748]

14. Schindelin J, Arganda-Carreras I, Frise E, Kaynig V, Longair M, Pietzsch T, et al. Fiji: an open-source platform for biological-image analysis. Nat Methods. 2012;9: 676–682. doi:10.1038/nmeth.2019 [PubMed: 22743772]

15. Schneider CA, Rasband WS, Eliceiri KW. NIH Image to ImageJ: 25 years of image analysis. Nat Methods. 2012;9: 671–675. doi:10.1038/nmeth.2089 [PubMed: 22930834]

16. Chollet F Keras: The python deep learning library. Astrophysics Source Code Library. 2018. Available: https://ui.adsabs.harvard.edu/abs/2018ascl.soft06022C/abstract

17. Abadi M, Agarwal A, Barham P, Brevdo E, Chen Z, Citro C, et al. TensorFlow: Large-Scale Machine Learning on Heterogeneous Distributed Systems. arXiv [cs.DC]. 2016. Available: http://arxiv.org/abs/1603.04467

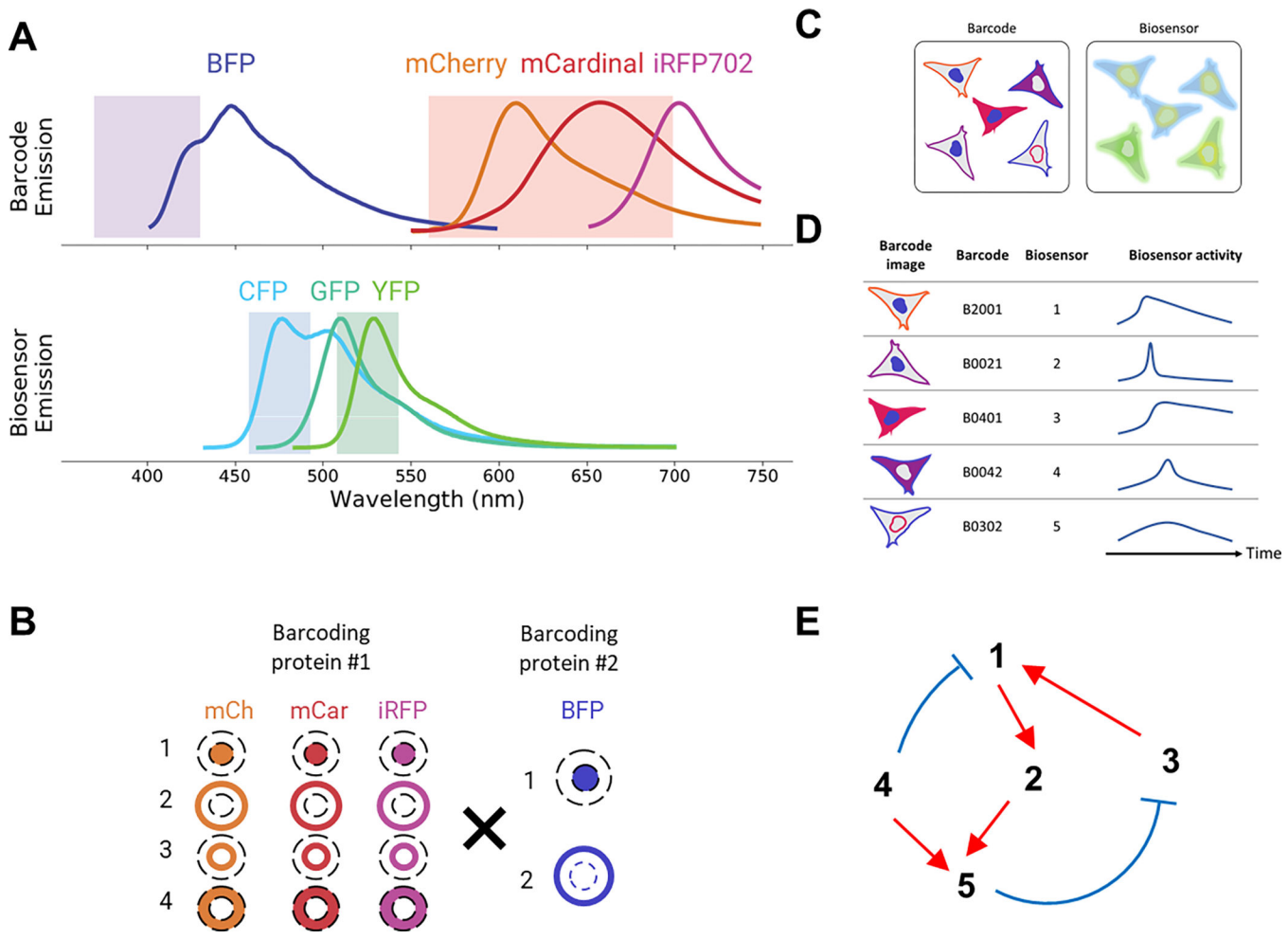

Figure 1. Overview of network reconstruction using biosensor barcoding.

(A) Emission spectrums of barcoding proteins and biosensors.

(B) Generation of barcodes from combinations of two barcoding proteins: the first based on a red FP and the second BFP.

(C) Cells are mixed for simultaneous imaging of barcodes and biosensors.

(D) The responses to biosensors to inhibitors are obtained from time-lapse images of biosensors, the identity of which can be determined by the barcodes expressed in the same cells.

(E) The interactions between the nodes can be deduced from the responses to inhibitors.

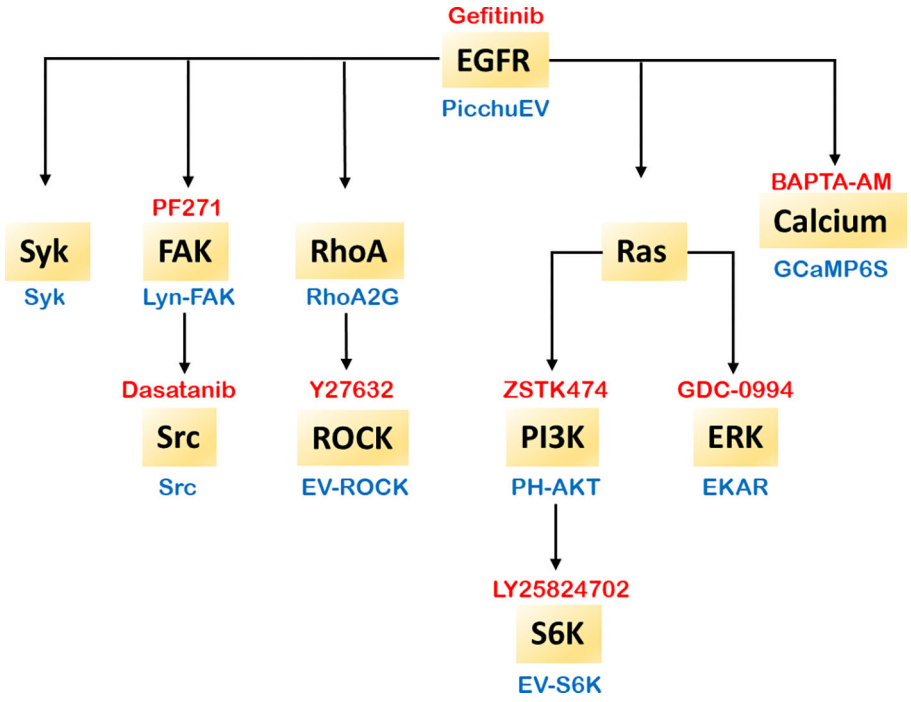

Figure 2. Biosensors and inhibitors for the EGFR signaling network.
The biosensors used in this chapter are shown in blue and inhibitors in red.

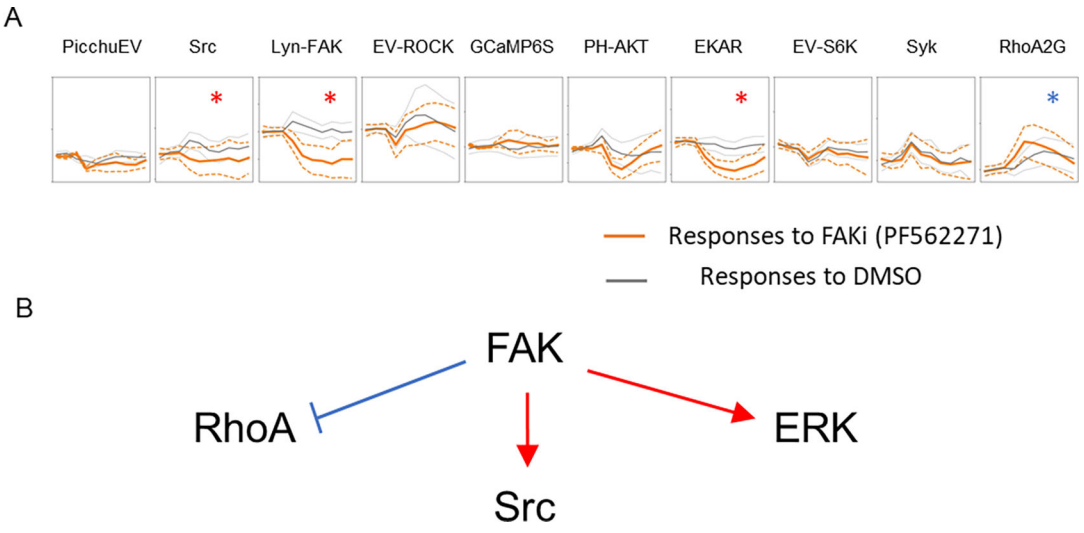

Figure 3. Inferring interactions from responses to inhibitors.

(A) Responses of biosensors to the FAK inhibitor PF-562271. Red and blue stars indicate statistically significant decrease and increase, respectively, in the activity induced by the FAKi (orange) when compared to the DMSO control (gray).

(B) Positive (red) and negative (blue) interactions between FAK and other nodes in the network can be inferred from a decreased or increased response, respectively, to the FAK inhibitor.

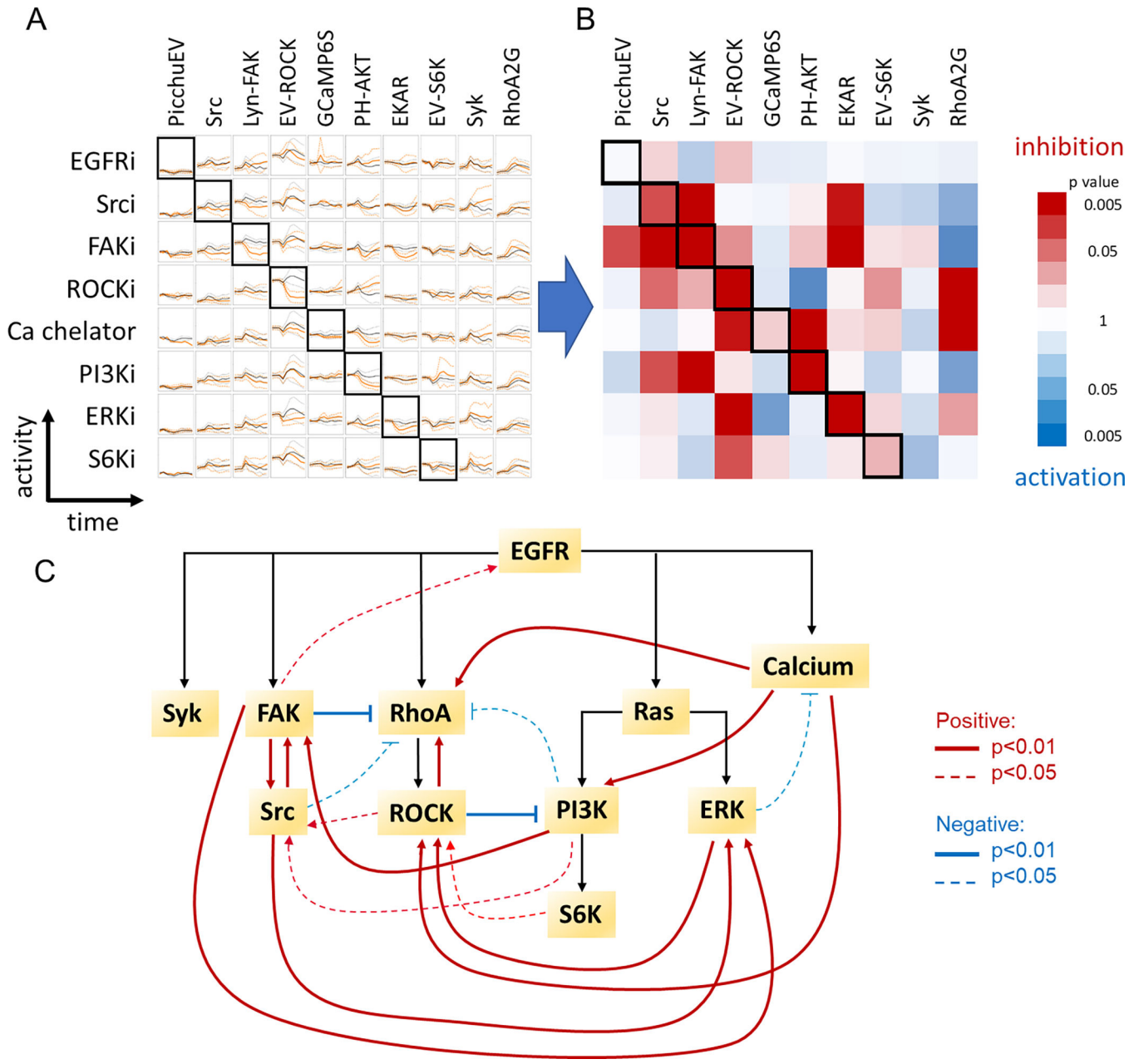

Figure 4. Constructing the interaction map.

(A) Responses of biosensors to inhibitors are displayed as traces in orange, while the traces in gray indicate the responses to the vehicle control.

(B) The matrix of inhibition displays how inhibitors affect the activities of biosensors. Red and blue colors indicate negative and positive effects, respectively, while the color scale indicates the statistical significance. Biosensors associated with the targets of inhibitors are indicated by black boxes.

(C) From the inhibition matrix, feedback loops are deduced by assigning positive (red) or negative (blue) interactions based on whether an inhibitor resulted in the inhibition or activation, respectively, of another node in the network.

Table 1.

Biosensors and barcodes

The biosensor and a pair of barcoding proteins are transfected into cells separately. Each barcode consists of a BFP (code: D) targeted to either the nuclear or plasma membrane, and one of the three red FPs: mCherry (E), mCardinal (B),or iRFP702 (C) targeted to one of four subcellular locations: the nucleus (1), plasma membrane (2), nuclear membrane (3), or cytosol (4). The barcode digits, from left to right, indicate the subcellular location of the targeted FPs: mCherry, mCardinal, iRFP702, and BFP, with 0 denoting not expressed. For instance, barcoding protein combination E2D1 represents mCherry at location 2 (plasma membrane) and BFP at location 1 (nucleus), with the corresponding barcode 3001.

Biosensor name	Target	Barcoding proteins	Barcode
PicchuEV	EGFR	B4D1	0401
Src biosensor	Src	E4D1	4001
Lyn-FAK	FAK	E3D1	3001
EV-ROCK	ROCK	C1D2	0012
GCaMP6S	Calcium	C2D1	0021
PH-AKT	PI3K	B1D1	0101
EKAR	ERK	B3D2	0302
EV-S6K	S6K	E2D1	2001
Syk biosensor	Syk	E2D2	2002
RhoA2G	RhoA	C4D2	0042

Table 2.

Inhibitors

Drug Name	Target	Stock Concentration (mM)	Working Concentration (μM)	Source	Identifier
Gefitinib	EGFR	1	1	Cayman	13166
PF562271	FAK	10	1	AdipoGen	SYN-1064
ZSTK474	PI3K	10	1	Cell Signaling	13213
GDC-0994	ERK	10	1	APExBIO Technology	B5817
BAPTA-AM	Calcium	10	10	Selleck	S7534
Y27632	ROCK	10	10	Enzo Life Sciences	ALX-270–333
Dasatinib	Src	10	1	Cayman	11498
LY2584702	S6K	1	1	Selleck	S7698

Table 3.

Imaging file templates and their purposes

Filename	Purpose
*[Experiment ID]*_405Ex.lsm	For generating barcodes: BFP channel (1-channel)
*[Experiment ID]*_633Ex.lsm	For spectral analysis: 15 bins
*[Experiment ID]*_633Ex_Linear unmixing.lsm	For generating barcodes: RFP channels (3-channel)
*[Experiment ID]*_FRET.lsm	For selecting ROIs and measuring CFP/YFP intensity (2-channel, time-lapse)